



Grid-Tied PV System With Small DC-Link Capacitor and Low-Frequency Ripple-Free Maximum Power Point Tracking

Archa Das¹, Raji Krishna², Lekshmisree V³

PG Student [Power System & Control], EEE, Govt. Engg College Bartonhill, Trivandrum, Kerala India ¹

Assistant Professor, EEE, Govt. Engg College Bartonhill, Trivandrum, Kerala India ²

Assistant Professor(Adhoc), EEE, Govt. Engg College Bartonhill, Trivandrum, Kerala India ³

Abstract—This paper proposes a grid-tied cascaded multilevel inverter (CMI) PV system based on current-fed dual-active-bridge (CF-DAB) dc-dc converters using small dc-link capacitors. The cascaded multilevel inverter (CMI) has many advantages, such as modularity, low harmonic spectra, high ac voltage application with low device rating and low electro-magnetic interference (EMI). In addition, distributed maximum power point tracking (MPPT) terminal for segmented PV arrays can be achieved by CMI PV converter. The low-frequency ripple-free MPPT is also realized in the proposed converter. A novel variable step-size MPPT algorithm is proposed to ensure high MPPT efficiency and fast maximum power extraction under rapid irradiation change. Fast tracking speed under rapid irradiation change and high MPPT efficiency were realized for the PV system.

Index Terms—Current-fed dual-active-bridge (CF-DAB), dual-active-bridge (DAB), high frequency link (HFL), low-frequency ripple, maximum power point tracking (MPPT).

I. INTRODUCTION

Photovoltaic (PV) energy has become one of the most popular sustainable energy sources nowadays. Global energy crises and environmental concerns from conventional fossil fuels have attracted more and more renewable energy developments in the worldwide. Among of these renewable energy, solar energy is much easier to be harvested, converted and delivered to grid by a variety of power converters. As a promising topology for grid-tied PV system, the cascaded multilevel inverter (CMI) has many advantages, such as modularity, high ac voltage application with low device rating, low harmonic spectra and low electromagnetic interference etc. In addition, distributed maximum power point tracking (MPPT) terminal for segmented PV arrays can be achieved by a CMI PV converter. The galvanic isolation between the PV panel and the grid is required to prevent electric shock on PV panel due to insulation damage and to suppress leakage current. Hence, compared to single-stage CMI converter, the cascaded multilevel inverter integrated with high frequency-link (HFL)-based dc-dc converter has advantage of providing galvanic isolation between the PV panel and the grid without using bulky line-frequency transformer. However, in a three-phase wye-connected CMI PV system with dc-dc stage, electrolytic capacitors are used as the dc-link energy buffers between dc-dc stage and inverter stage to provide the double-line frequency (2ω) power to the grid. Electrolytic capacitor which is an unreliable component, is on average 30 times less reliable than non electrolytic capacitor under identical conditions. Therefore, capacitance reduction is highly desirable in order to achieve high reliability with non electrolytic film capacitor, especially for the high-voltage CMI PV system. The small dc-link capacitance will make the converter suffer from large double frequency voltage ripple on the dc-link. If this voltage ripple propagates to the PV side, it will deteriorate the MPPT performance and decrease the MPPT efficiency. Current-fed isolated dc-dc converters can be used to solve this issue. It has inherent advantages over the voltage-fed types because the input current of current-fed converter can be controlled directly, and thus, it is possible to eliminate the input low-frequency power ripple in the PV side by special designed current control.

II. SYSTEM CONFIGURATION AND LOW FREQUENCY RIPPLE POWER

Fig. 1 presents the system configuration of a proposed MW scale grid-tied PV system with CF-DAB dc-dc converters. It consists of i cascaded multilevel inverter modules for each phase and each inverter module is connected to j cascaded CF-DAB converter modules. Compared with traditional PV systems, this system shows many advantages. Because of



the high-frequency isolated dc–dc converters, the PV system can be directly connected to the high-voltage ac grid without bulky line-frequency transformer, and the converter output voltage is scalable due to the modular structure. Each dc–dc module is interfaced with segmented PV arrays having independent MPPT; therefore, the solar energy harvesting can be maximized. Moreover, flexible control strategies are able to be explored and applied in this topology. By using the reactive power compensation and optimization strategy, the proposed converter can reduce the over modulation of the PV inverter output voltage caused by unsymmetrical active power generation from PV arrays, and thus, improve the system power quality and reliability. In addition, due to the isolated CF-DAB converter, the ground leakage current is effectively suppressed. Particularly, this converter can reduce the dc-link capacitance and enable film capacitor implementation by allowing large voltage ripple on the dc-link; hence, the PV system reliability is greatly improved. The dc-link capacitance is mainly determined by the allowed voltage ripple on the dc-link in specific system. For the PV system in Fig. 1, the instantaneous power flow through each phase leg contains 2ω fluctuating power. The dc-link capacitance required to buffer the energy can be calculated by

$$C_{dc1a} = \frac{S_{1p}}{\omega_g \Delta V_{dc1a} V_{dc1a}}$$

where S_{1p} is the apparent output power flow through the single phase leg, ω_g is line frequency, V_{dc1a} and ΔV_{dc1a} are the average voltage and the allowed peak-to-peak ripple voltage on the dc-link, respectively.

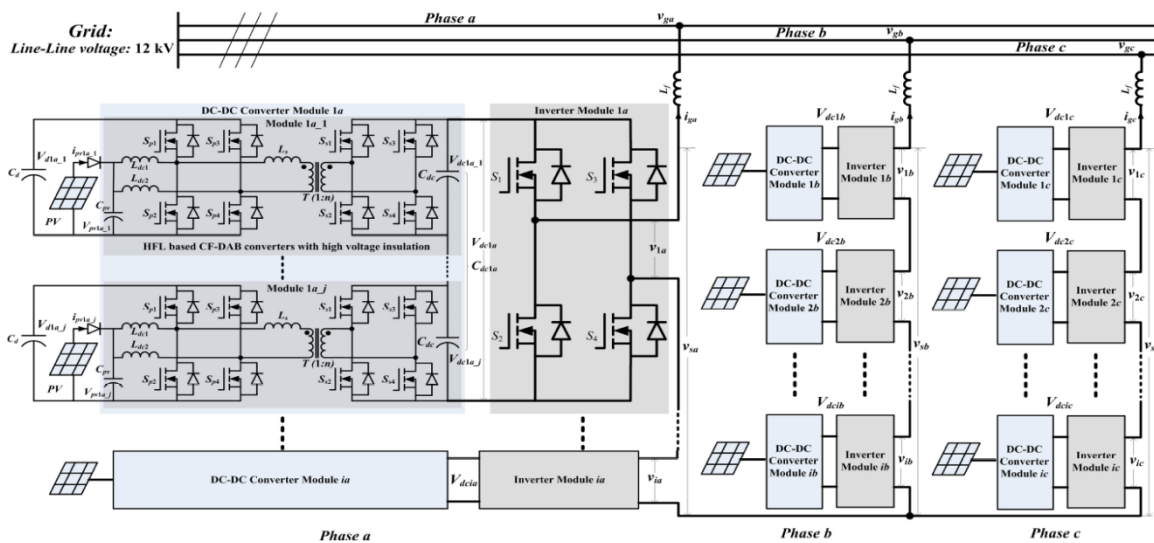


Fig. 1. Grid-tied cascaded multilevel PV inverter system based on CF-DAB dc-dc converters.

The required dc-link capacitance is inversely proportional to the dc-link voltage and the allowed voltage ripple. With selected bus voltage, small capacitance will result in large voltage ripple on the capacitor. This large low frequency voltage ripple on the dc-link imposes challenges on the PV system operation, especially on the dc–dc stage. The ripple significantly increases the peak current inside the CF-DAB converter module if unbalanced bus voltage occurs between primary side and secondary side. Moreover, this large 2ω voltage ripple can decrease the MPPT efficiency if it propagates to PV side. Fig. 2 illustrates how the low-frequency voltage ripple affects the PV power generation.

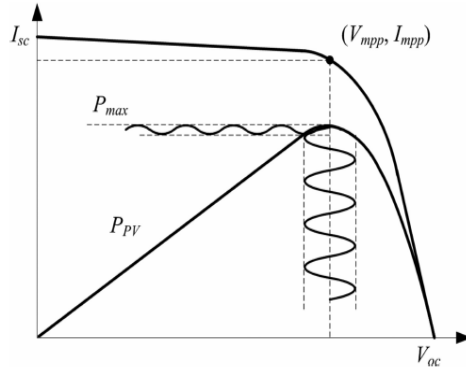


Fig. 2. Low-frequency ripple effect on the MPPT.

It can be seen that the PV output power will be typically diminished from the maximum power at (V_{mpp}, I_{mpp}) if the PV voltage or current has low-frequency ripple. The voltage ripple should be kept below 8.5% to get 98% utilization factor of PV array. With the CF-DAB dc-dc converter interface adopted in this paper, the low-frequency voltage ripple can be effectively attenuated in the PV side through the power mitigation control, thus large voltage ripple on dc-link is allowed without influence on the PV power. With low-frequency ripple-free PV voltage, high effective MPPT become possible. Using the autonomous variable step size MPPT strategy, the proposed PV system can achieve high efficient MPPT in steady state and fast tracking under rapid irradiation change.

III. LOW FREQUENCY POWER MITIGATING CONTROL

A PV system including one single dc-dc module and one inverter module, namely $i=1$ and $j=1$ of Fig. 1 is selected for analysis. The dc-link voltage v_{dc} is controlled by the inverter module. Duty-cycle plus phase-shift control is employed for the CF-DAB converter. The PV voltage v_{pv} is regulated by the duty cycle D , while the low voltage side (LVS) voltage v_d is controlled by the phase-shift angle ϕ . To minimize the peak current of the transformer, “ $d = 1$ ” control using PI + Resonant (PIR) controller is applied to synchronize the LVS and high voltage side (HVS) dc-link voltage. A low-frequency power mitigation strategy using dual-loop control with dc-link voltage fed forward is developed for the PV voltage control.

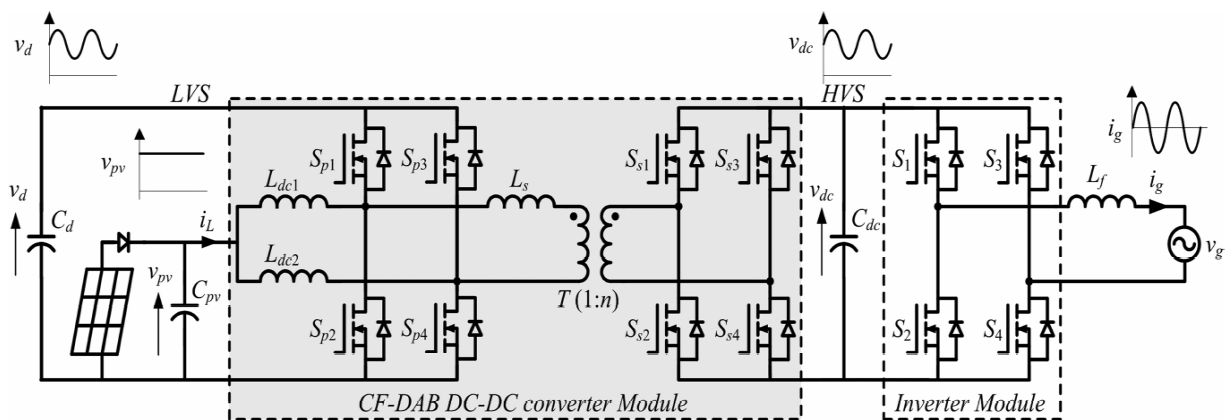


Fig. 3. PV system including one single dc-dc module and one inverter module

The PV voltage v_{pv} and the inductor current i_L are used to calculate the PV voltage variation dv_{pv} , PV power p_{pv} , and PV power variation dp_{pv} . And the PV voltage reference v_{pv}^* is generated from MPPT block, which is implemented with an



autonomous variable step-size MPPT strategy that can achieve high efficiency and fast MPPT under rapid irradiation change.

IV. VARIABLE STEP SIZE MPPT WITH FAST TRACKING

The proposed variable step-size MPPT strategy based on an INC method is sketched in Fig. 4. dv_{pv} , di_{pv} , dp_{pv} , and p_{pv} are first calculated using the filtered PV voltage and inductor current to avoid sensing noise in the circuit. Then, according to dp_{pv} , the step-size algorithm is divided into two separate paths.

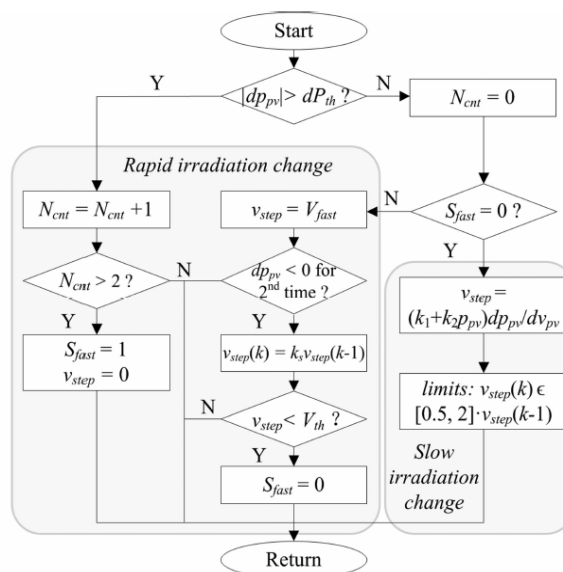


Fig 4. Variable step-size INC algorithm

If the changed power is above the threshold dp_{th} for two times in succession, rapid irradiation change mode is detected, otherwise the converter continues with step-size calculation in slow irradiation change mode. Fig. 5 shows the operating paths of the INC method under rapid irradiation change.

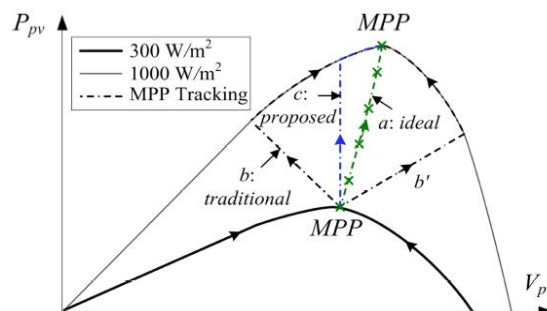


Fig. 5. Operating paths of INC MPPT method under rapid irradiation change.

During rapid irradiation change, the operating PV curves change dramatically. Ideally, if the PV converter can follow the operating path *a*, all the available power can be extracted from the PV array. However, this extra power change due to irradiation variation may confuse the MPPT algorithm, which may lead to MPPT failure and energy waste as



illustrated in operating path b and b' . To avoid possible MPPT failure, the PV voltage is kept unchanged as long as the rapid irradiation change is detected, as shown in operating path c . Since the MPP voltage does not vary much for different irradiation level, this unchanged PV voltage is close to new MPP voltage; therefore, most of the power generated can still be extracted. Once the irradiation change become slowly, a large MPPT step V_{fast} will be used at first for fast tracking of the new MPP. After the new MPP is crossed twice, the voltage step size is scaled down by factor k_s in each MPPT cycle. When the step size is smaller than V_{th} , the MPPT exits the rapid irradiation change mode, switching to slow irradiation change mode. With this algorithm, the energy waste during rapid irradiation change is reduced, and the system achieves fast tracking under rapid irradiation change without failure.

V. SIMULINK MODEL AND SIMULATION RESULTS

Fig 6 represents the Simulink model of CFDAB converter. The simulation of the proposed CFDAB converter is performed in MATLAB 2016a/Simulink and it is compared with the conventional DAB converter. Fig 7 and fig 8 represents the simulation output of DAB converter and CFDAB converter respectively. From the output waveform it is clear that settling time of CFDAB converter is less compared to DAB converter. And CFDAB converter has higher output voltage compared to DAB converter. Fig 9 represents the simulation output of CFDAB converter with controller. The characteristics of CFDAB converter includes inherent zero-voltage switching (ZVS), high step-up ratio, interleaved structure, and wide input voltage capability. Fig 10 represents the simulation output of three phase inverter.

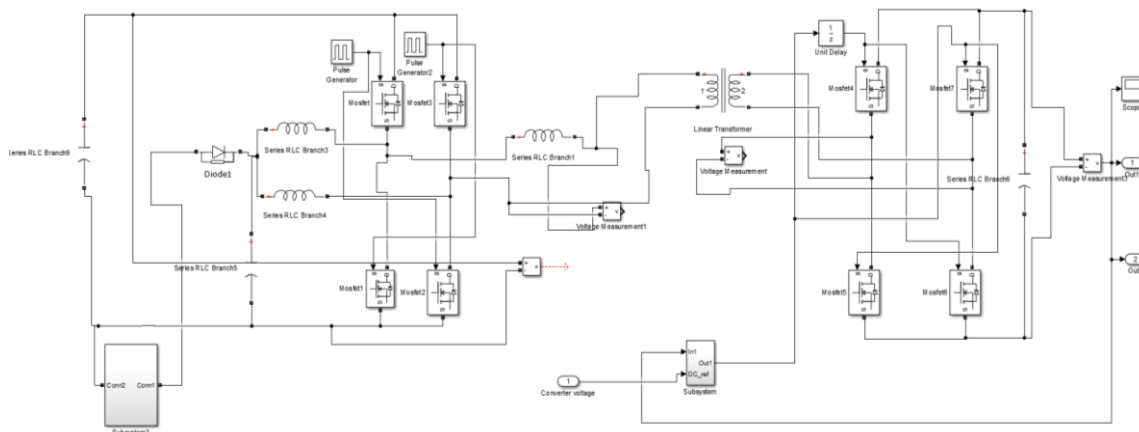


Fig 6. Simulink model of CFDAB converter

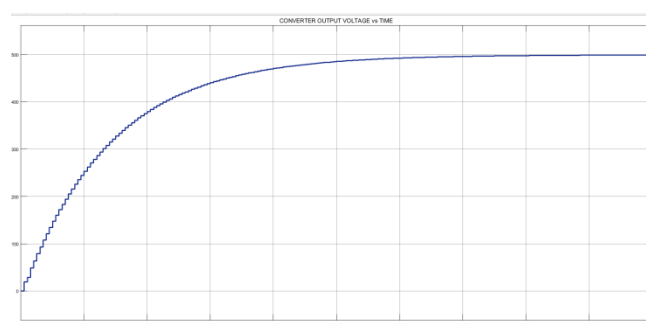


Fig 7. Simulation output of DAB converter

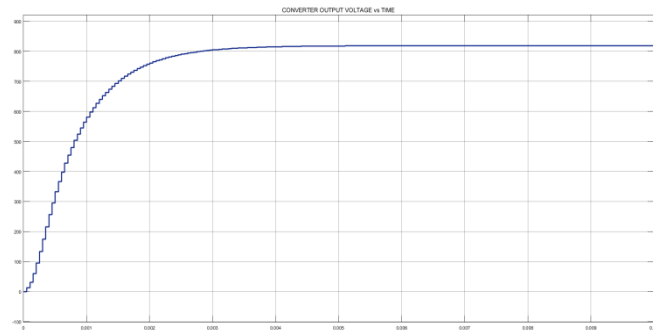


Fig 8. Simulation output of CFDAB converter without controller

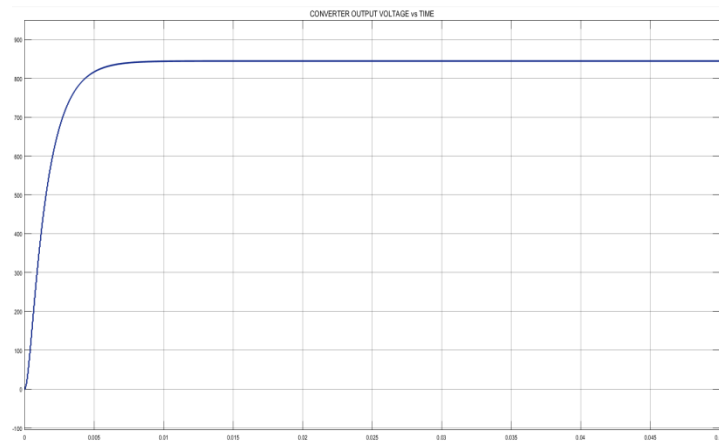


Fig 9. Simulation output of CFDAB converter with controller

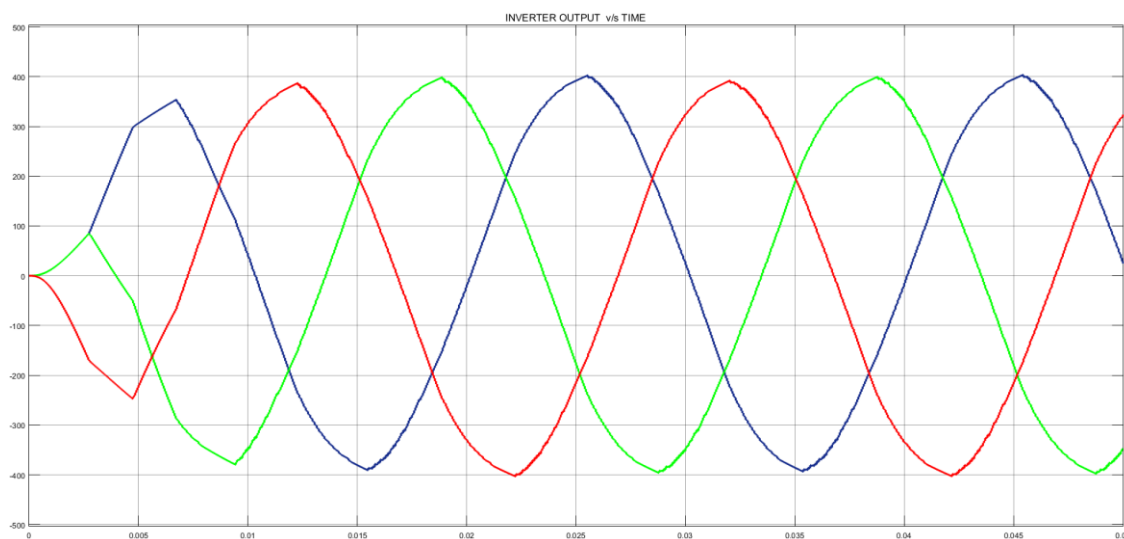


Fig 10. Simulation output of inverter with controller



VI. CONCLUSION

In this paper, a grid-tied CMI PV system based on CF-DAB dc-dc converters using small dc-link capacitors has been proposed. A dc link synchronising control is applied to minimize the peak current stress in the converter by synchronizing the LVS dc link voltage with HVS dc-link voltage. The 2ω ripple on the input PV voltage can be greatly attenuated by using low-frequency power mitigation control. This proposed power mitigation control can be extended to other current-fed topologies, e.g., CF-DHB and CF-DAB3. A variable step-size INC MPPT with an adaptive scaling factor is used to improve tracking speed during rapid irradiation change.

REFERENCES

- [1] B. K. Bose, "Global warming: Energy, environmental pollution, and the impact of power electronics," *IEEE Ind. Electron. Mag.*, vol. 4, no. 1, pp. 6–17, Mar. 2010.
- [2] Y. Shi, L. Liu, H. Li, and Y. Xue, "A single-phase grid-connected PV converter with minimal dc-link capacitor and low-frequency ripple-free maximum power point tracking," in *Proc. IEEE Energy Convers. Congr. Expo.*, Sep. 2013, pp. 2385–2390.
- [3] F. Liu, S. Duan, F. Liu, B. Liu, and Y. Kang, "A variable step size INC MPPT method for PV systems," *IEEE Trans. Ind. Electron.*, vol. 55, no. 7, pp. 2622–2628, Jul. 2008.
- [4] Q. Mei, M. Shan, L. Liu, and J. M. Guerrero, "A novel improved variable step-Size incremental-resistance MPPT method for PV systems," *IEEE Trans. Ind. Electron.*, vol. 58, no. 6, pp. 2427–2434, Jun. 2011.
- [5] L. Liu, H. Li, Y. Xue, and W. Liu, "Reactive power compensation and optimization strategy for grid-interactive cascaded photovoltaic systems," *IEEE Trans. Power Electron.*, vol. 10, no. 1, pp. 188–202, Jan. 2015.
- [6] L. Liu, H. Li, Y. Xue, and W. Liu, "Decoupled active and reactive power control for large-scale grid-connected photovoltaic systems using cascaded modular multilevel converters," *IEEE Trans. Power Electron.*, vol. 10, no. 1, pp. 176–187, Jan. 2015.
- [7] M. Malinowski, K. Gopakumar, J. Rodriguez, and M. A. Perez, "A survey on cascaded multilevel inverters," *IEEE Trans. Ind. Electron.*, vol. 57, no. 7, pp. 2197–2206, Jul. 2010.
- [8] C. Sullivan, J. Awerbuch, and A. Latham, "Decrease in photovoltaic power output from ripple: Simple general calculation and the effect of partial shading," *IEEE Trans. Power Electron.*, vol. 28, pp. 740–747, Feb. 2013.
- [9] H. Tao, J. L. Duarte, and M. A. M. Hendrix, "Three-port triple-half-bridge bidirectional converter with zero-voltage switching," *IEEE Trans. Power Electron.*, vol. 23, no. 2, pp. 782–792, Mar. 2008.
- [10] Renewable Energy Policy Network, (2014, Apr.). Renewables 2014 global status report. [Online]. Available: <http://www.ren21.net/ren21activities/globalstatusreport.aspx>.
- [11] S. Harb and R. S. Balog, "Reliability of candidate photovoltaic module-integrated-inverter (PV-MII) topologies—A usagemodel approach," *IEEE Trans. Power Electron.*, vol. 28, no. 6, pp. 3019–3027, Jun. 2013.
- [12] H. Hu, S. Harb, N. Kutkut, I. Batarseh and Z. John Shen, "Power decoupling techniques for micro-inverters in PV systems—A review," in *Proc. IEEE Energy Convers. Congr. Expo.*, Sep. 2010, pp. 3235–3240.
- [13] "Reliability prediction for electronic equipment," United States Dept. Defence, Washington, DC, USA, Doc. MIL-HDBK-217X, Dec. 1991.
- [14] G. Petrone, G. Spagnuolo, R. Teodorescu, M. Veerachary, and M. Vitelli, "Reliability issues in photovoltaic power processing systems," *IEEE Trans. Ind. Electron.*, vol. 55, no. 7, pp. 2569–2580, Jul. 2008.